

Proposal for measuring new transverse momentum dependent parton distributions g_{1T} and h_{1L}^\perp through semi-inclusive deep inelastic scattering

Jiacai Zhu^a, Bo-Qiang Ma^{a,b,*}

^a*School of Physics and State Key Laboratory of Nuclear Physics and Technology, Peking University, Beijing 100871, China*

^b*Center for High Energy Physics, Peking University, Beijing 100871, China*

Abstract

We calculate g_{1T} and h_{1L}^\perp , two of the eight leading twist transverse momentum dependent parton distributions (TMDs), in the light-cone quark-diquark model. The new TMDs can be measured through semi-inclusive deep inelastic scattering (SIDIS). We present predictions of the single and double spin asymmetries related to g_{1T} and h_{1L}^\perp in SIDIS at HERMES, COMPASS, and JLab kinematics respectively.

Keywords: transverse momentum dependent parton distributions, light-cone quark-diquark model, semi-inclusive deep inelastic scattering, spin asymmetry

1. Introduction

Transverse momentum dependent parton distributions (TMDs) [1, 2], as a generalization of parton distribution functions (PDFs) from one dimension to three dimensions in momentum space, provide rich information on nucleon structure. At leading twist, there are eight TMDs contained in the quark-

*Corresponding author.

Email address: mabq@pku.edu.cn (Bo-Qiang Ma)

quark correlation matrix [3, 4]:

$$\begin{aligned} \Phi(x, \mathbf{k}_T) = \frac{1}{2} \left\{ f_1 \not{\epsilon}_+ - f_{1T} \frac{\epsilon_T^{ij} k_{Ti} S_{Tj}}{M_N} \not{\epsilon}_+ + \left(S_L g_{1L} + \frac{\mathbf{k}_T \cdot \mathbf{S}_T}{M_N} g_{1T} \right) \gamma_5 \not{\epsilon}_+ \right. \\ \left. + h_{1T} \frac{[\not{\epsilon}_T, \not{\epsilon}_+] \gamma_5}{2} + \left(S_L h_{1L} + \frac{\mathbf{k}_T \cdot \mathbf{S}_T}{M_N} h_{1T}^\perp \right) \frac{[k_T, \not{\epsilon}_+] \gamma_5}{2M_N} \right. \\ \left. + i h_1^\perp \frac{[k_T, \not{\epsilon}_+]}{2M_N} \right\}. \end{aligned} \quad (1)$$

Using the notation $\Phi^{[\Gamma]} \equiv \text{Tr}(\Phi\Gamma)/2$, one gets

$$\Phi^{[\gamma^+]} = f_1(x, k_T^2) - S_{Tj} \frac{\epsilon_T^{ij} k_{Ti}}{M_N} f_{1T}^\perp(x, k_T^2), \quad (2)$$

$$\Phi^{[\gamma^+ \gamma_5]} = S_L g_{1L}(x, k_T^2) + \frac{\mathbf{k}_T \cdot \mathbf{S}_T}{M_N} g_{1T}(x, k_T^2), \quad (3)$$

$$\begin{aligned} \Phi^{[i\sigma^{i+} \gamma_5]} = S_T^i h_1(x, k_T^2) + S_L \frac{k_T^i}{M_N} h_{1L}^\perp(x, k_T^2) - S_{Tj} \frac{2k_T^i k_T^j + k_T^2 g_T^{ij}}{2M_N^2} h_{1T}^\perp(x, k_T^2) \\ - \frac{\epsilon_T^{ij} k_{Tj}}{M_N} h_1^\perp(x, k_T^2), \quad i = 1, 2, \end{aligned} \quad (4)$$

where $h_1(x, k_T^2) = h_{1T}(x, k_T^2) + (k_T^2/2M_N^2)h_{1T}^\perp(x, k_T^2)$. If we integrate over transverse momenta \mathbf{k}_T , these three correlation functions $\Phi^{[\gamma^+]}$, $\Phi^{[\gamma^+ \gamma_5]}$, and $\Phi^{[i\sigma^{i+} \gamma_5]}$ reduce to the unpolarized, helicity, and transversity distributions respectively, while other five TMDs vanish.

Among the eight TMDs, g_{1T} and h_{1L}^\perp are probably the least considered ones. Besides, they reflect new information on the quark spin and orbital correlation of the nucleon. g_{1T} describes the probability of finding a longitudinally polarized quark inside a transversely polarized nucleon, so we could call it transversal helicity (or shortly, trans-helicity). In the same manner, h_{1L}^\perp could be called longitudinal transversity (or shortly, longi-transversity or heli-transversity) for that it represents the probability of finding a transversely polarized quark inside a longitudinally polarized nucleon. The unique feature of g_{1T} and h_{1L}^\perp is that for other six TMDs, there are corresponding generalized parton distributions (GPDs) in the light-cone quark models, but for g_{1T} and h_{1L}^\perp , the corresponding GPDs vanish because of time invariance [5].

h_{1L}^\perp is chiral-odd, so it can be probed via SIDIS when combined with the chiral-odd Collins fragmentation function. For g_{1T} , it is chiral-even,

and can be measured through SIDIS when combined with the unpolarized fragmentation function.

2. g_{1T} and h_{1L}^\perp in the light-cone quark-diquark model

In the light-cone quark-diquark model [6, 7], if any one of the quarks in the proton is struck, the other parts of the proton can be effectively treated as a spectator with its quantum numbers being those of a diquark with spin 0 or 1 (scalar and vector diquarks). Moreover, the Melosh-Wigner rotation [8, 9], which plays an important role to explain the proton spin puzzle [10, 11] due to the relativistic effect of quark transversal motions, is taken into account in the model. In Ref. [12], the pretzelosity distribution h_{1T}^\perp was calculated in the light-cone quark-diquark model. Following the same method with the proper selections of the proton polarization directions, we get the expressions of g_{1T} and h_{1L}^\perp in the light-cone quark-diquark model:

$$\begin{aligned} g_{1T}^{(uv)} &= -\frac{1}{16\pi^3} \times \left(\frac{1}{9} \sin^2 \theta_0 \varphi_V^2 W_V^g - \cos^2 \theta_0 \varphi_S^2 W_S^g \right), \\ g_{1T}^{(dv)} &= -\frac{1}{8\pi^3} \times \frac{1}{9} \sin^2 \theta_0 \varphi_V^2 W_V^g, \end{aligned} \quad (5)$$

and

$$\begin{aligned} h_{1L}^{\perp(uv)} &= -\frac{1}{16\pi^3} \times \left(\frac{1}{9} \sin^2 \theta_0 \varphi_V^2 W_V^h - \cos^2 \theta_0 \varphi_S^2 W_S^h \right), \\ h_{1L}^{\perp(dv)} &= -\frac{1}{8\pi^3} \times \frac{1}{9} \sin^2 \theta_0 \varphi_V^2 W_V^h, \end{aligned} \quad (6)$$

with the Melosh-Wigner rotation factors ($D = V, S$):

$$W_D^g(x, k_T^2) = \frac{2M_N(x\mathcal{M}_D + m_q)}{(x\mathcal{M}_D + m_q)^2 + k_T^2}, \quad (7)$$

$$W_D^h(x, k_T^2) = -\frac{2M_N(x\mathcal{M}_D + m_q)}{(x\mathcal{M}_D + m_q)^2 + k_T^2}, \quad (8)$$

where

$$\mathcal{M}_D = \sqrt{\frac{m_q^2 + k_T^2}{x} + \frac{m_D^2 + k_T^2}{1-x}}. \quad (9)$$

$\varphi_D(D = V, S)$ is the wave function in the momentum space for the quark-diquark, and for which we can use the Brodsky-Huang-Lepage (BHL) prescription [13, 14]:

$$\varphi_D(x, k_T^2) = A_D \exp \left\{ -\frac{1}{8\alpha_D^2} \left[\frac{m_q^2 + k_T^2}{x} + \frac{m_D^2 + k_T^2}{1-x} \right] \right\}. \quad (10)$$

The parameters $\alpha_D = 0.33$ GeV, the quark mass $m_q = 0.33$ GeV, the diquark mass $m_S = 0.60$ GeV, $m_V = 0.80$ GeV, and $\theta_0 = \pi/4$ are adopted for numerical calculation. θ_0 is the mixing angle that breaks the SU(6) symmetry when $\theta_0 \neq \pi/4$.

The unpolarized distributions, in the light-cone quark-diquark model, can be found in Refs. [6, 7]:

$$\begin{aligned} f_1^{(uv)}(x, k_T^2) &= \frac{1}{16\pi^3} \left(\frac{1}{3} \sin^2 \theta_0 \varphi_V^2 + \cos^2 \theta_0 \varphi_S^2 \right), \\ f_1^{(dv)}(x, k_T^2) &= \frac{1}{8\pi^3} \frac{1}{3} \sin^2 \theta_0 \varphi_V^2. \end{aligned} \quad (11)$$

Using Eqs. (5), (6), and (11), one can express g_{1T} and h_{1L}^\perp with the unpolarized distributions:

$$\begin{aligned} g_{1T}^{(uv)}(x, k_T^2) &= [f_1^{(uv)}(x, k_T^2) - \frac{1}{2} f_1^{(dv)}(x, k_T^2)] W_S^g(x, k_T^2) - \frac{1}{6} f_1^{(dv)}(x, k_T^2) W_V^g(x, k_T^2), \\ g_{1T}^{(dv)}(x, k_T^2) &= -\frac{1}{3} f_1^{(dv)}(x, k_T^2) W_V^g(x, k_T^2), \end{aligned} \quad (12)$$

and

$$\begin{aligned} h_{1L}^{\perp(uv)}(x, k_T^2) &= [f_1^{(uv)}(x, k_T^2) - \frac{1}{2} f_1^{(dv)}(x, k_T^2)] W_S^h(x, k_T^2) - \frac{1}{6} f_1^{(dv)}(x, k_T^2) W_V^h(x, k_T^2), \\ h_{1L}^{\perp(dv)}(x, k_T^2) &= -\frac{1}{3} f_1^{(dv)}(x, k_T^2) W_V^h(x, k_T^2). \end{aligned} \quad (13)$$

From Eqs. (7) and (8), one gets the following relation:

$$g_{1T}^{(qv)}(x, k_T^2) = -h_{1L}^{\perp(qv)}(x, k_T^2), \quad (14)$$

which is supported in other models [15, 16, 17, 18]. With expressions of h_1 in Refs. [19, 20] and h_{1T}^\perp in Ref. [12], we get

$$\frac{1}{2} [h_{1L}^{\perp(qv)}(x, k_T^2)]^2 \geq -h_1^{(qv)}(x, k_T^2) h_{1T}^{\perp(qv)}(x, k_T^2), \quad (15)$$

where the two sides are equal only if $q = d$. This is different from what has been obtained in other models [17, 18], where the two sides are equal for both $q = u$ and $q = d$.

3. g_{1T} and h_{1L}^\perp related asymmetries in semi-inclusive deep inelastic scattering

g_{1T} and h_{1L}^\perp can be measured via the double and single spin asymmetries in the SIDIS process respectively [21, 22]. There have been also other proposals to measure g_{1T} through other process [23] and h_{1L}^\perp through SIDIS [24, 25]. The cross section of the SIDIS process reads:

$$\frac{d\sigma}{dx dy d\psi dz d\phi_h dP_{h\perp}^2} = \frac{\alpha^2}{xy Q^2} \frac{y^2}{2(1-\varepsilon)} \left(1 + \frac{\gamma^2}{2x}\right) \left\{ F_{UU,T} + S_L \varepsilon \sin(2\phi_h) F_{UL}^{\sin 2\phi_h} + S_T \lambda_e \sqrt{1-\varepsilon^2} \cos(\phi_h - \phi_S) F_{LT}^{\cos(\phi_h - \phi_S)} + \dots \right\}, \quad (16)$$

and other terms will not contribute in our analysis below. Using notations $\hat{\mathbf{h}} \equiv \mathbf{P}_{h\perp}/P_{h\perp}$ and

$$\mathcal{F}[w(\mathbf{k}_T, \mathbf{p}_T) f D] = x \sum_q e_q^2 \int d\mathbf{k}_T d\mathbf{p}_T \delta^{(2)}(\mathbf{k}_T - \mathbf{p}_T - \mathbf{P}_{h\perp}/z) \times w(\mathbf{k}_T, \mathbf{p}_T) [f^q(x, k_T^2) D^q(z, p_T^2) + f^{\bar{q}}(x, k_T^2) D^{\bar{q}}(z, p_T^2)], \quad (17)$$

one has

$$F_{UU,T} = \mathcal{F}[f_1 D_1], \quad (18)$$

$$F_{LT}^{\cos(\phi_h - \phi_S)} = \mathcal{F}\left[\frac{\hat{\mathbf{h}} \cdot \mathbf{k}_T}{M_N} g_{1T} D_1\right], \quad (19)$$

$$F_{UL}^{\sin 2\phi_h} = \mathcal{F}\left[-\frac{2(\hat{\mathbf{h}} \cdot \mathbf{p}_T)(\hat{\mathbf{h}} \cdot \mathbf{k}_T) - \mathbf{p}_T \cdot \mathbf{k}_T}{M_N M_h} h_{1L}^\perp H_1^\perp\right]. \quad (20)$$

We define the asymmetries related to g_{1T} and h_{1L}^\perp as

$$A_{LT}^{\cos(\phi_h - \phi_S)} = \frac{F_{LT}^{\cos(\phi_h - \phi_S)}}{F_{UU,T}}, \quad (21)$$

$$A_{UL}^{\sin 2\phi_h} = \frac{F_{UL}^{\sin 2\phi_h}}{F_{UU,T}}. \quad (22)$$

We present numerical calculations in two different approaches: for approach 1, we use Eqs. (5) and Eqs. (6) directly to calculate; while for approach 2, we adopt the CTEQ6L parametrization [26] for the unpolarized

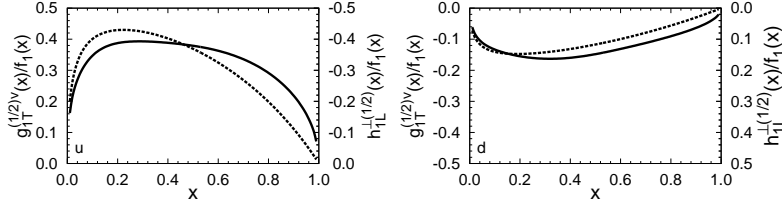


Figure 1: The ratios $g_{1T}^{(1/2)v}(x)/f_1(x)$ and $h_{1L}^{\perp(1/2)v}(x)/f_1(x)$. Dashed curves correspond to approach 1, while solid curves correspond to approach 2. Left for u quark, and right for d quark.

distributions, assume a Gaussian form factor of transverse momentum as suggested in Ref. [27]:

$$f_1(x, k_T^2) = f_1(x) \frac{\exp(-k_T^2/k_{av}^2)}{\pi k_{av}^2} \quad (23)$$

with $k_{av}^2 = 0.25 \text{ GeV}^2$, and then use Eqs. (12) and Eqs. (13) to calculate. The ratios $g_{1T}^{(1/2)v}(x)/f_1(x)$ and $h_{1L}^{\perp(1/2)v}(x)/f_1(x)$ are shown in Fig. 1 with $Q^2 = 3.0 \text{ GeV}^2$, where the notation

$$j^{(1/2)}(x) = \int d\mathbf{k}_T \left(\frac{k_T^2}{2M_N^2} \right)^{1/2} j(x, k_T^2) \quad (24)$$

for TMD $j(x, k_T^2)$ is used. For the unpolarized and Collins fragmentation functions, we adopt the forms suggested in the same paper [27], and the parametrization of $D_1(z)$ can be found in Ref. [28]. When we calculate the asymmetries, we only sum over the valence quark distributions in approach 1, while in approach 2, the unpolarized quark and antiquark distributions are considered. As we mentioned in Ref. [12], approach 2 involves the CTEQ6L parametrization which has been well verified and constrained by many experiments, and can give more reasonable predictions for future experiments.

Now, we present the predictions of the double spin asymmetry $A_{LT}^{\cos(\phi_h - \phi_S)}$ and the single spin asymmetry $A_{UL}^{\sin 2\phi_h}$ in SIDIS at different kinematics as shown in Table. 1. Both π^+ and π^- productions of the proton target in HERMES [29, 30], COMPASS [31, 32] and JLab [33, 34] experiments, the neutron target in COMPASS and JLab experiments, and the deuteron target in HERMES and COMPASS experiments are calculated. The results for the double spin asymmetry $A_{LT}^{\cos(\phi_h - \phi_S)}$ are shown in Figs. 2 3 4, and those for the single spin asymmetry $A_{UL}^{\sin 2\phi_h}$ are shown in Figs. 5 6 7, respectively.

Table 1: Kinematics at HERMES, COMPASS and JLab

	HERMES	COMPASS	JLab6		JLab12	
			proton	neutron	proton	neutron
$p_{\text{lab}}/\text{GeV}$	27.6	160	6	6	12	12
Q^2/GeV^2	> 1	> 1	> 1	1.3–3.1	> 1	> 1
W^2/GeV^2	> 10	> 25	> 4	5.4–9.3	> 4	> 2.3
x	0.023–0.4		0.1–0.6	0.13–0.4	0.05–0.7	0.05–0.55
y	0.1–0.85	0.1–0.9	0.4–0.85	0.68–0.86	0.2–0.85	0.34–0.9
z	0.2–0.7	0.2–1	0.4–0.7	0.46–0.59	0.4–0.7	0.3–0.7

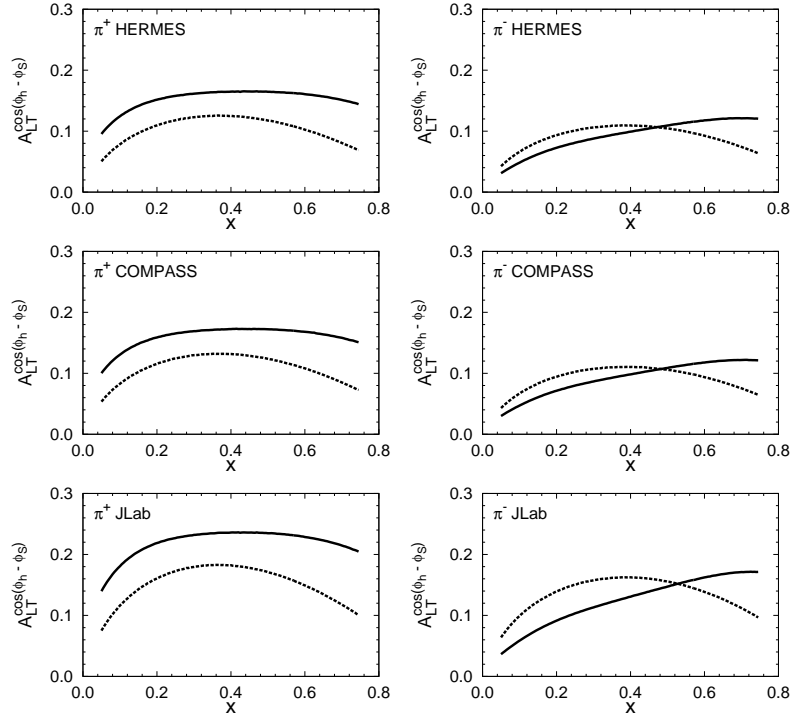


Figure 2: The double spin asymmetry $A_{LT}^{\cos(\phi_h - \phi_S)}$ as a function of x at different kinematics with $Q^2 = 3.0 \text{ GeV}^2$ for the proton target. Dashed curves correspond to approach 1, while solid curves correspond to approach 2.

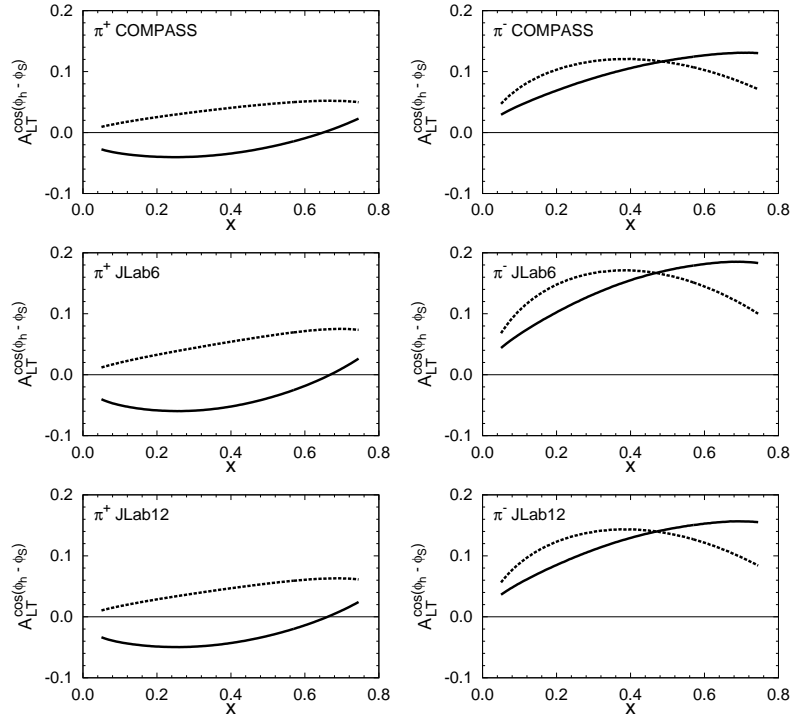


Figure 3: The double spin asymmetry $A_{LT}^{\cos(\phi_h - \phi_S)}$ as a function of x at different kinematics with $Q^2 = 3.0 \text{ GeV}^2$ for the neutron target. Dashed curves correspond to approach 1, while solid curves correspond to approach 2.

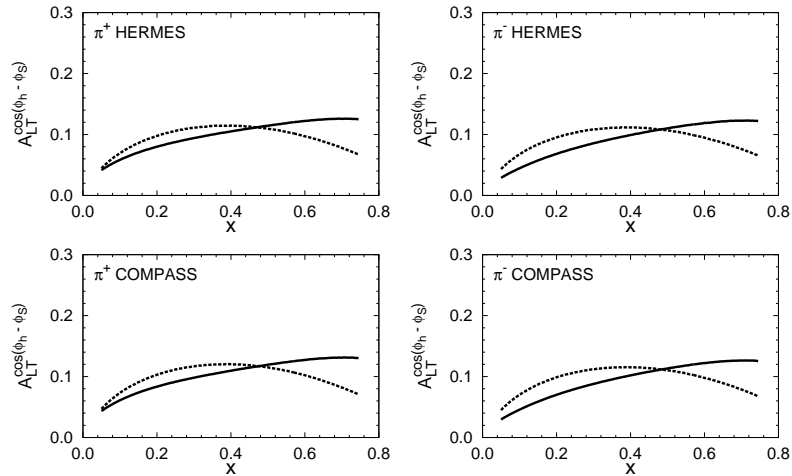


Figure 4: The double spin asymmetry $A_{LT}^{\cos(\phi_h - \phi_S)}$ as a function of x at different kinematics with $Q^2 = 3.0 \text{ GeV}^2$ for the deuteron target. Dashed curves correspond to approach 1, while solid curves correspond to approach 2.

The magnitudes of these asymmetries are significantly larger compared with those of the single spin asymmetry $A_{UT}^{\sin(3\phi_h - \phi_S)}$ that we obtained in Ref. [12], so a transverse momentum cut is not necessary. The magnitudes of our results are comparable with those in Ref. [35] but larger than those in Ref. [36].

4. Summary

We have calculated two of the eight leading twist TMDs, g_{1T} and h_{1L}^\perp , in the light-cone quark-diquark model, and found some interesting relations among them. They can be measured through SIDIS. The predictions of the double and single asymmetries in SIDIS related to them have been presented at HERMES, COMPASS and JLab kinematics for the proton, neutron and deuteron targets. We expect future experiments can prompt our understanding of the nucleon spin structure.

Acknowledgments

This work is supported by National Natural Science Foundation of China (Nos. 10721063, 10975003, and 11035003).

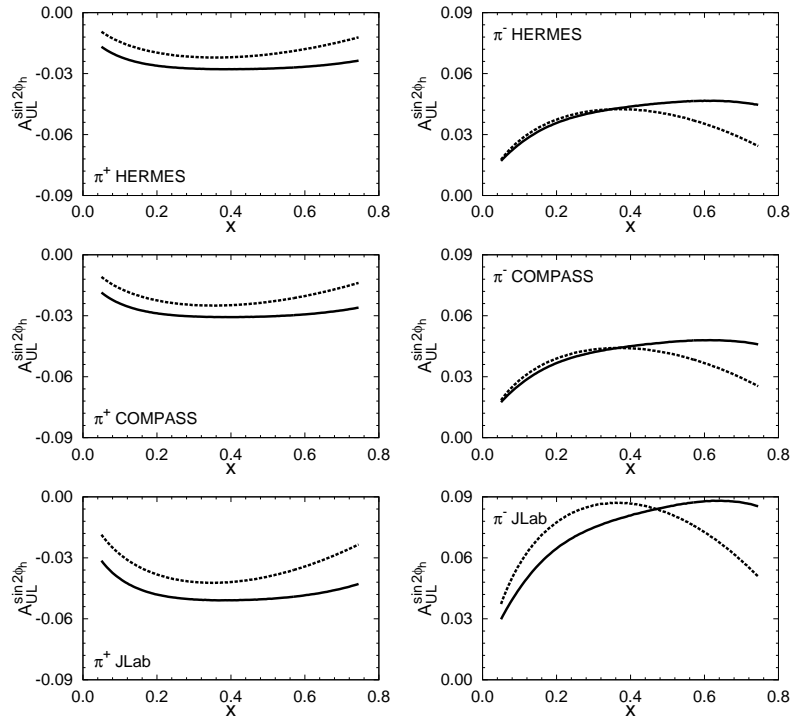


Figure 5: The single spin asymmetry $A_{UL}^{\sin 2\phi_h}$ as a function of x at different kinematics with $Q^2 = 3.0 \text{ GeV}^2$ for the proton target. Dashed curves correspond to approach 1, while solid curves correspond to approach 2.

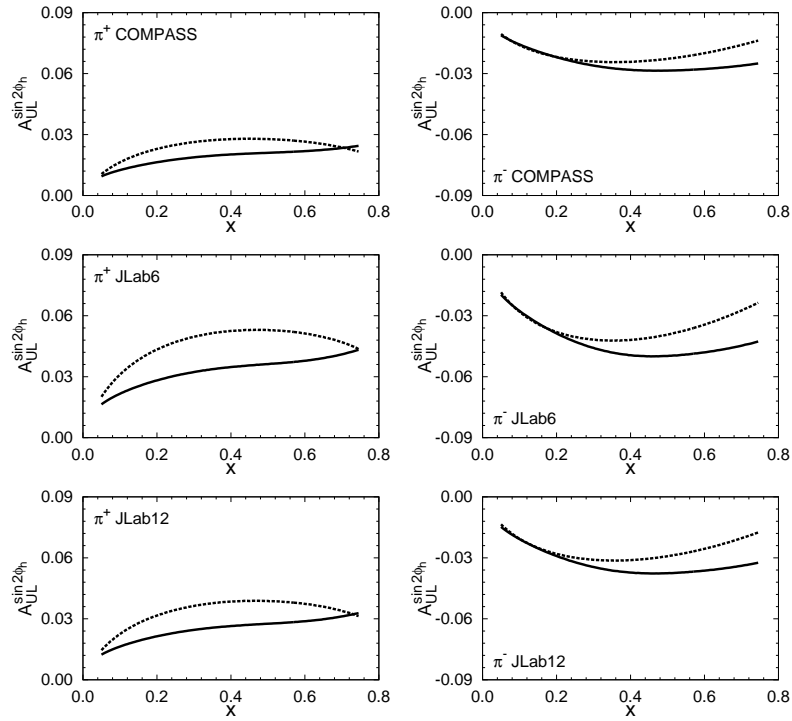


Figure 6: The single spin asymmetry $A_{UL}^{\sin 2\phi_h}$ as a function of x at different kinematics with $Q^2 = 3.0 \text{ GeV}^2$ for the neutron target. Dashed curves correspond to approach 1, while solid curves correspond to approach 2.

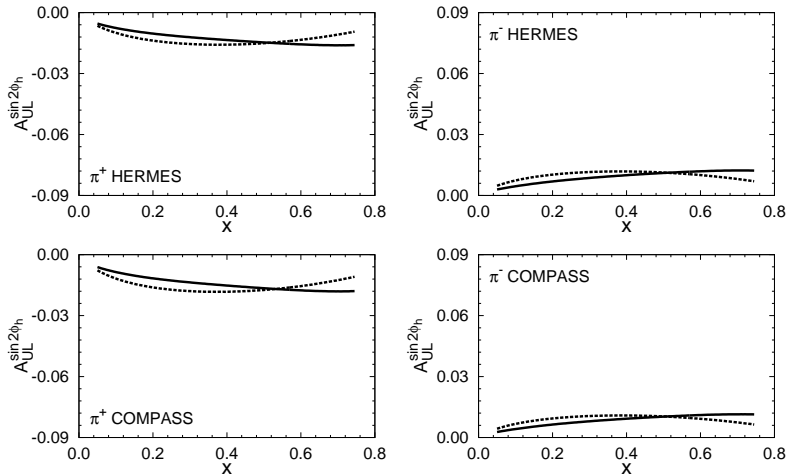


Figure 7: The single spin asymmetry $A_{UL}^{\sin 2\phi_h}$ as a function of x at different kinematics with $Q^2 = 3.0 \text{ GeV}^2$ for the deuteron target. Dashed curves correspond to approach 1, while solid curves correspond to approach 2.

References

- [1] V. Barone, A. Drago, P. G. Ratcliffe, Phys. Rept. 359 (2002) 1.
- [2] V. Barone, F. Bradamante, A. Martin, Prog. Part. Nucl. Phys. 65 (2010) 267.
- [3] P. J. Mulders, R. D. Tangerman, Nucl. Phys. B461 (1996) 197.
- [4] D. Boer, P. J. Mulders, Phys. Rev. D57 (1998) 5780.
- [5] M. Diehl, P. Hagler, Eur. Phys. J. C44 (2005) 87.
- [6] B.-Q. Ma, Phys. Lett. B375 (1996) 320.
- [7] B.-Q. Ma, I. Schmidt, J. Soffer, J.-J. Yang, Phys. Rev. D62 (2000) 114009.
- [8] E. P. Wigner, Annals Math. 40 (1939) 149.
- [9] H. J. Melosh, Phys. Rev. D9 (1974) 1095.
- [10] B.-Q. Ma, J. Phys. G17 (1991) L53, [arXiv:0711.2335].

- [11] B.-Q. Ma, Z. Phys. C58 (1993) 479.
- [12] J. She, J. Zhu, B.-Q. Ma, Phys. Rev. D79 (2009) 054008.
- [13] S. J. Brodsky, T. Huang, and G. P. Lepage, in *Quarks and Nuclear Forces*, edited by D. Fries and B. Zeitnitz (Springer, Tracts in Modern Physics, Vol. 100) (Springer, New York, 1982).
- [14] T. Huang, B.-Q. Ma, Q.-X. Shen, Phys. Rev. D49 (1994) 1490.
- [15] R. Jakob, P. J. Mulders, J. Rodrigues, Nucl. Phys. A626 (1997) 937.
- [16] B. Pasquini, S. Cazzaniga, S. Boffi, Phys. Rev. D78 (2008) 034025.
- [17] A. V. Efremov, P. Schweitzer, O. V. Teryaev, P. Zavada, Phys. Rev. D80 (2009) 014021.
- [18] H. Avakian, A. V. Efremov, P. Schweitzer, F. Yuan, Phys. Rev. D81 (2010) 074035.
- [19] I. Schmidt, J. Soffer, Phys. Lett. B407 (1997) 331.
- [20] B.-Q. Ma, I. Schmidt, J. Soffer, Phys. Lett. B441 (1998) 461.
- [21] A. Kotzinian, Nucl. Phys. B441 (1995) 234.
- [22] A. Bacchetta, M. Diehl, K. Goeke, A. Metz, P. J. Mulders, M. Schlegel, JHEP 02 (2007) 093.
- [23] Z. Lu, B.-Q. Ma, I. Schmidt, Phys. Rev. D75 (2007) 094012.
- [24] B.-Q. Ma, I. Schmidt, J.-J. Yang, Phys. Rev. D63 (2001) 037501.
- [25] B.-Q. Ma, I. Schmidt, J.-J. Yang, Phys. Rev. D65 (2002) 034010.
- [26] J. Pumplin, D. R. Stump, J. Huston, H. L. Lai, P. M. Nadolsky, W. K. Tung, JHEP 07 (2002) 012.
- [27] M. Anselmino, M. Boglione, U. D'Alesio, A. Kotzinian, F. Murgia, A. Prokudin, S. Melis, Nucl. Phys. B (Proc. Suppl.) 191 (2009) 98.
- [28] D. de Florian, R. Sassot, M. Stratmann, Phys. Rev. D75 (2007) 114010.
- [29] A. Airapetian, et al., Phys. Rev. Lett. 94 (2005) 012002.

- [30] A. Airapetian, et al., Phys. Lett. B693 (2010) 11.
- [31] V. Y. Alexakhin, et al., Phys. Rev. Lett. 94 (2005) 202002.
- [32] M. G. Alekseev, et al., Phys. Lett. B692 (2010) 240.
- [33] JLab E06-010/E06-011, X. Jiang, J. P. Chen, E. Cisbani, H. Gao, and J. C. Peng, spokespersons.
- [34] H. Gao, et al., arXiv:1009.3803.
- [35] A. Kotzinian, B. Parsamyan, A. Prokudin, Phys. Rev. D73 (2006) 114017.
- [36] S. Boffi, A. V. Efremov, B. Pasquini, P. Schweitzer, Phys. Rev. D79 (2009) 094012.